The Astrophysical Journal, 591:L61–L65, 2003 July 1

PROBING THE EDGE OF THE SOLAR SYSTEM: FORMATION OF AN UNSTABLE JET-SHEET

Merav Opher,[1] Paulett C. Liewer,[1] Tamas I. Gombosi,[2] Ward Manchester,[2]
Darren L. DeZeeuw,[2] Igor Sokolov,[2] and Gabor Toth[2,3]
Received 2003 January 8; accepted 2003 May 19; published 2003 June 9

ABSTRACT

The *Voyager* spacecraft is now approaching the edge of the solar system. Near the boundary between the solar system and the interstellar medium we find that an unstable "jet-sheet" forms. The jet-sheet oscillates up and down because of a velocity shear instability. This result is due to a novel application of a state-of-the-art three-dimensional MHD code with a highly refined grid. We assume as a first approximation that the solar magnetic and rotation axes are aligned. The effect of a tilt of the magnetic axis with respect to the rotation axis remains to be seen. We include in the model self-consistently magnetic field effects in the interaction between the solar and interstellar winds. Previous studies of this interaction had poorer spatial resolution and did not include the solar magnetic field. This instability can affect the entry of energetic particles into the solar system and the intermixing of solar and interstellar material. The same effect found here is predicted for the interaction of rotating magnetized stars possessing supersonic winds and moving with respect to the interstellar medium, such as O stars.

Subject headings: instabilities — interplanetary medium — ISM: kinematics and dynamics — MHD — solar wind — Sun: magnetic fields

On-line material: mpeg animations

1. INTRODUCTION

Our solar system presents a unique local example of the interaction between a stellar wind and the interstellar medium. As the Sun travels through the interstellar medium, it is subject to an interstellar wind. Three different discontinuities are formed because of the interaction between the supersonic solar wind flow and the interstellar wind: termination shock, heliopause, and, in the case where the interstellar wind is supersonic, a bow shock. At the termination shock, the supersonic solar wind passes to a subsonic regime. The heliopause is a tangential discontinuity that separates the charged components of the two winds. Beyond the termination shock, the solar wind velocity is no longer constant but decreases with radial distance until it reaches the heliopause. A bow shock may form in the interstellar wind since observations indicate that the solar system travels with a supersonic velocity of approximately 25 km s^{-1} (Frisch 1996). The complex system created by the interaction of the solar wind with the interstellar wind is known as the *global heliosphere*.

In recent years, there has been increased interest in heliospheric studies in modeling the solar and interstellar interaction, in part because of the two successful *Voyager* missions, launched in 1977 and early 2003, at 87 and 69 AU. There is the expectation that in the near future the *Voyager* spacecraft, traveling toward the heliopause, will cross the termination shock (Stone, Cummings, & Webber 1996). Accurate modeling of this region will allow us to interpret the data taken during the passage of *Voyager* through (and beyond) the termination shock (for a review on the subject see Suess 1990). Recent works include elaborate computational models (Baranov & Malama 1993; Pauls, Zank, & Williams 1995; Pauls & Zank 1996; Zank et al. 1996; Müller, Zank, & Lipatov 2000; Liewer, Karmesin, & Brackbill 1996; Pogorelov & Matsuda 2000; Linde et al. 1998; Izmodenov, Gruntman, & Malama 2001; Washimi & Tanaka 1996, 2001). Nearly all the models, however, ignore magnetic field effects, especially the solar magnetic field. While the solar magnetic field does not play a major dynamic role in the interplanetary region (Linde et al. 1998), this is not true beyond the termination shock. In the present Letter, we focus on the interaction region between the solar wind and the interstellar medium, paying special attention to the region beyond the termination shock.

The solar magnetic field, under quiet solar conditions, is approximately a dipole with opposite polarities in the north and south hemispheres. The supersonic solar wind pulls the solar field out into space, creating a *heliospheric current sheet* separating magnetic field regions of opposite polarities. The heliospheric current sheet corresponds to the region where the azimuthal field $B_\phi = 0$. In the present study we neglect the tilt of the magnetic field axis with respect to the rotation axis. Therefore, near the Sun the current sheet remains at the equatorial plane. An important question overlooked in previous studies is the fate of the current sheet beyond the termination shock. Previous numerical studies by Linde et al. (1998) and Washimi & Tanaka (1996, 2001), which used a three-dimensional MHD simulation that included both the solar and interstellar magnetic field, reported results indicating that the current sheet beyond the termination shock remains in the equatorial plane. These studies also neglected the tilt of the magnetic axis with respect to the rotation axis.

The rotation of the Sun coupled to a supersonic solar wind twists the interplanetary magnetic field lines such that the magnetic field, upstream of the termination shock (toward the Sun), takes the shape of an Archimedian spiral (known as the Parker field; Parker 1958). In analytic studies of the region beyond the termination shock, Nerney, Suess, & Schmahl (1991, 1993) predicted the presence of *magnetic ridges* due to the compression of the azimuthal interplanetary field. Their studies were made in the kinematic approximation where the magnetic field back-reaction on the flow was neglected. The flow plasma

[1] Jet Propulsion Laboratory, MS 169-506, 4800 Oak Grove Drive, Pasadena, CA 91109; merav.opher@jpl.nasa.gov.
[2] Space Physics Research Laboratory, Department of Atmospheric, Oceanic, and Space Sciences, University of Michigan, Ann Arbor, MI 48109.
[3] Eötvös University, Department of Atomic Physics, Budapest, Hungary.

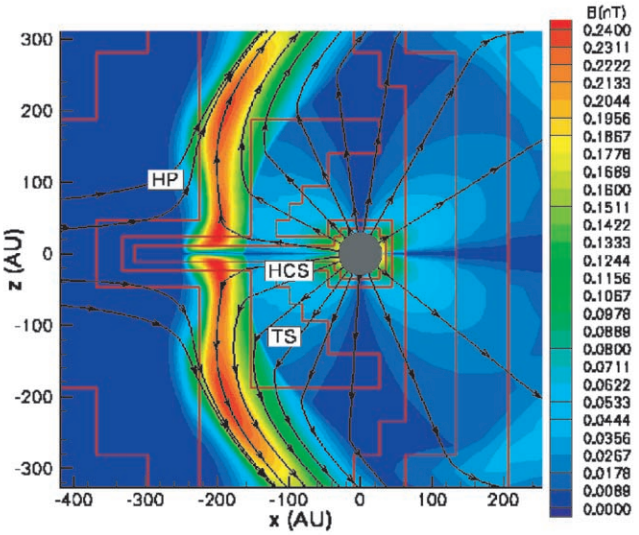

FIG. 1.—Contours of the magnetic field at $t = 32$ yr (scale ranging from 0 to 0.24 nT) in the meridional plane (x-z). The z-axis is parallel to the solar rotation. The red lines indicate the boundaries when the grid refinement changes. The HP, TS, and heliocurrent sheet (HCS) are indicated. Also are shown the flow streamlines (*black lines*). Note the solar dipolar magnetic field.

β_V (the ratio of solar wind ram to magnetic pressures) decreases by a factor of 10^3 near the stagnation point, indicating that a full MHD calculation in the region is necessary. Since there is no natural symmetry in the system, a three-dimensional calculation is required. The enormous range of scales, from hundreds of AU to less than 1 AU at the current sheet, requires a time-dependent adaptive grid code, making the calculation computationally very challenging.

2. SIMULATION RESULTS

2.1. *Description of the Model*

We used a full three-dimensional MHD adaptive grid code, BATS-R-US, developed at the University of Michigan. This is a parallel multiprocessor code that employs an upwind finite-volume scheme based on an approximate Riemann solver for MHD. The single-fluid MHD equations are solved in a fully three-dimensional coupled manner. BATS-R-US makes use of a block-based adaptive grid that allows the model to resolve structures of widely varying length scales (see Powell et al. 1999; Gombosi et al. 2002).

The inner boundary of our calculation was placed at 30 AU, and the outer boundary was on a 3000 AU × 3000 AU × 2400 AU box. The grid was designed to resolve in detail the region between the termination shock and the heliopause, especially refining at the current sheet. We used 4.5 million cells ranging from scales of 1 AU at the current sheet to 36 AU at the outer boundary, with six levels of refinement. The parameters of the solar wind at the inner boundary were $n = 7.8 \times 10^{-3}$ cm^{-3}, $T = 1.6 \times 10^3$ K, and a magnetic field of $B = 2$ μG at the equator. For the interstellar medium, we used (Frisch 1996) $n = 0.07$ cm^{-3}, $v = 25$ km s^{-1}, and $T = 10^4$ K. The solar wind velocity at the inner boundary was assumed to be isotropic, with $v = 450$ km s^{-1}. The magnetic field for the solar system at the inner boundary was taken to be a Parker spiral (with the polarity of the solar magnetic field corresponding to this field being antiparallel to the axis of solar rotation). In order to eliminate the effect of reconnection at the heliopause in the present study, we did not include an interstellar magnetic field. Only the ionized component was treated.

2.2. *Formation of a "Jet-Sheet"*

Figure 1 is a meridional cut (x-z) at $t = 35$ yr showing the contours of the magnetic field. The calculation was initiated at $t = 0$, when the interstellar wind has reached the solar wind and the bow shock, heliopause, and termination shock have formed with the current sheet in the equatorial plane. The coordinate system is such that the interstellar wind is flowing from the negative x-direction and the solar rotation axis is in the positive z-direction. We observe at $x \simeq -210$ AU the presence of magnetic ridges (*red*), where the magnetic field increases to values of 2.4 μG.

Beyond the termination shock (TS), we find that a "jet-sheet" forms. As the flow decelerates beyond the TS, approaching the heliopause (HP), it compresses the azimuthal magnetic field, producing the magnetic ridges. In the current-sheet region, because of the absence of an azimuthal magnetic component, there is no magnetic pressure to slow down the flow, and the solar wind streams freely. This leads to the formation of a *jet* in the meridional plane and *sheet* in the equatorial plane. Because of the shear between the flow in the jet-sheet and the flow in the surrounding medium, the jet-sheet (and the current sheet) becomes unstable. We are the first to report this phenomena.

Figure 2*a* is a meridional cut at $t = 35$ yr showing the velocity contours between TS and the HP. We can see the jet structure: in the equatorial region the wind velocity is much faster than the surrounding medium. The red contours with positive velocities ($U_x \approx 20$ km s^{-1}) indicate solar wind material that was pushed aside by the jet and is flowing toward the TS. This produces the turbulence shown in the black lines that follow the flow streamlines. It can be seen that at $x = -210$ AU, the flow streams at the equator with a velocity of ≈130 km s^{-1}, while the surrounding medium flows with a velocity of 40 km s^{-1}. The flow in the current sheet at the TS is subject to the de Laval nozzle effect (Landau & Lifshitz 1987). As the nozzle widens (at $x = -180$ AU) the flow velocity increases, becoming supersonic, and then decreases approaching the HP. The sonic Mach number v/c_S, where v is the flow velocity and c_S is the sound velocity, is 1.1 at $x = -180$ AU, decreasing to 0.2 at $x = -300$ AU. Figure 2*c* shows a line plot of the velocity in the equatorial plane at $t = 35$ yr. Figure 3 shows the time evolution of the current sheet for nine different times. By $t = 71$ yr, the current sheet starts to bend toward positive z-values while the nose moves toward negative z-values. This bending increases the turbulence beneath the current sheet. The current sheet, after an initial bending to the south, reverses its direction and moves to the north. At later times, the HP is highly distorted, as can be seen by the flow streamlines in the bottom right panel of Figure 3. The flow in the HP is very complicated: more than one stagnation point occurs above the equator, and the two fluids appear to intermix. Figure 4 shows a three-dimensional image of the magnetic field contours and lines at $t = 346$ yr.

2.3. *Kelvin-Helmholtz–like Instability*

Because of the velocity shear between the jet-sheet and the surrounding medium, a Kelvin-Helmholtz–like (KH) instability develops. The KH growth rate, for an infinitely thin layer, is (Chandrasekhar 1961) $\Gamma = 0.5 \mid kU_0 \mid [1 - (2c_A \hat{\boldsymbol{k}} \cdot \hat{\boldsymbol{B}}_0)^2 / (\hat{\boldsymbol{k}} \cdot U_0)^2]^{1/2}$, where U_0 is the velocity jump across the shear layer, c_A is the Alfvén speed, $\hat{\boldsymbol{k}}$ is the direction of the wavevector

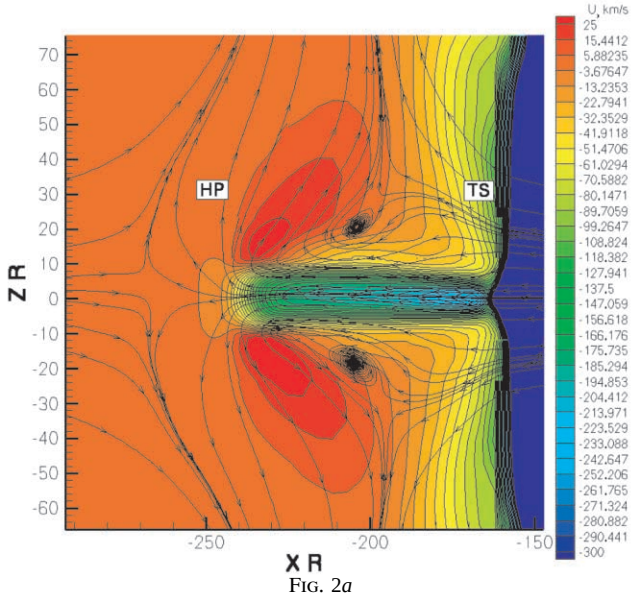

FIG. 2*a*

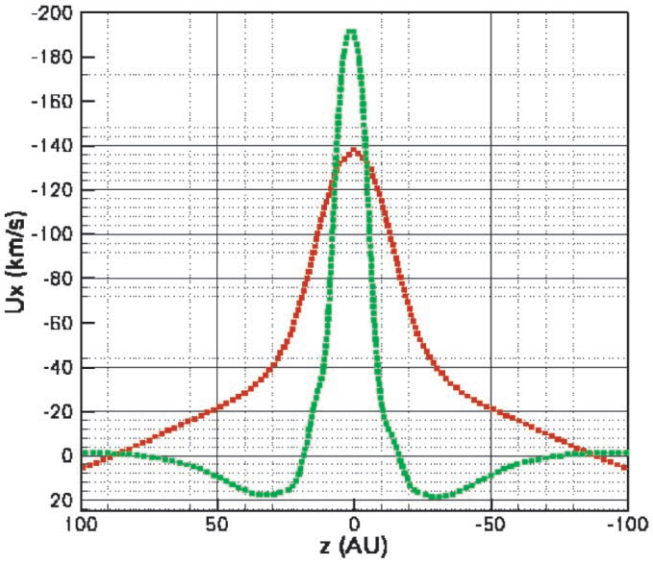

FIG. 2*b*

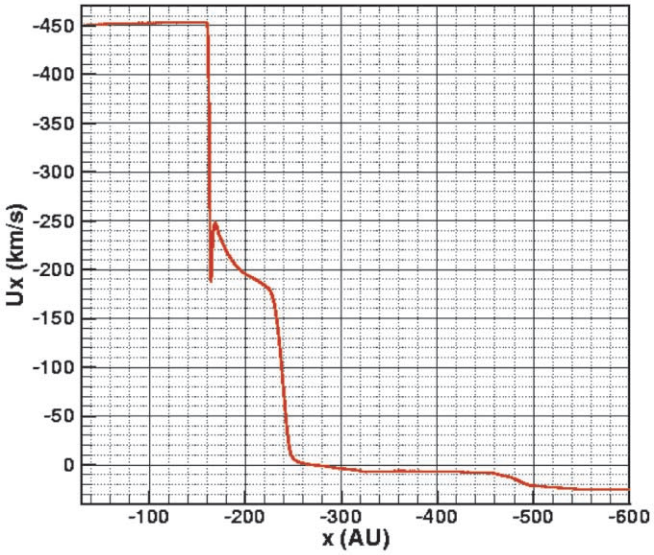

FIG. 2*c*

FIG. 2.—(*a*) Contours of the velocity U_x at $t = 35$ yr (scale ranging from -300 to 25 km s^{-1}) between TS and the HP in the meridional plane (x-z). (*b*) Line plots of the vertical cuts of U_x velocity from $z = -100$ to $z = 100$ AU at $x = -210$ AU (also at $t = 35$ yr). The refined grid (actual grid) is shown in green, and the coarser grid (see text) is shown in red. (*c*) Line plot of the equatorial cut at $t = 35$ yr of the velocity U_x vs. x. The TS is at $x = -160$ AU, the HP is at $x = -230$ AU, and the bow shock is at $x = -460$ AU. [Panel *a* is also available as an mpg animation in the electronic edition of the Journal.]

(here $\hat{\boldsymbol{x}}$), and $\hat{\boldsymbol{B}}_0$ is the direction of the magnetic field. Maximum growth occurs for $k \approx 1/a$; a is defined as the distance between the maximum velocity and zero (see Fig. 2*b*). For $t = 32$ yr for example, at $x = -210$ AU, $U_0 \approx 100$ km s^{-1} and $a \approx 20$ AU. With these values the predicted KH growth rate is 3.3×10^{-8} s^{-1}. The necessary condition for the KH instability is $c_A < | U_0/2B_0 |$. At $x = -210$ AU, $c_A/U_0 < 0.5$ for $| z | < 2$ AU, so the instability can occur near (and at) the current sheet. Measuring the displacement of the current sheet with respect to the equator at $x = -210$ AU during the evolution of the instability gives a linear growth rate of 1.6×10^{-9} s^{-1} (between $t = 0$ and 126 yr), comparable to the estimate for the KH instability in slab geometry. The wavelength of the perturbation $\lambda_x \approx 2\pi/k \approx 63$ AU, using $k \approx 1/a$, is also consistent with our results.

To determine whether this instability was not observed in prior studies because of the coarseness of the grid, we made an identical calculation using a less refined grid at the current sheet. For the coarse grid, the cell size at the current sheet was 4–6 AU, compared with the refined grid of 1 AU. No instability was seen. The current sheet remained in the equator, consistent with the previous numerical calculations (e.g., Washimi & Tanaka 1996 used a spherical grid with a resolution varying from $\Delta R \approx 6$ AU to $\Delta R \approx 20$ AU from the inner to the outer boundary). The line plot in Figure 2*b* compares the velocity profiles for our coarse and the refined grid cases. For the coarse grid, the velocity of the jet is 4 times wider (≈30 AU half-width) and smaller by a factor of 2. The linear KH growth rate $\Gamma \propto kU_0$, and thus we expect a decrease of about a factor of 8. The instability is apparently suppressed in the coarse grid case not only because the growth rate decreases but also because numerical dissipative effects wash it out.

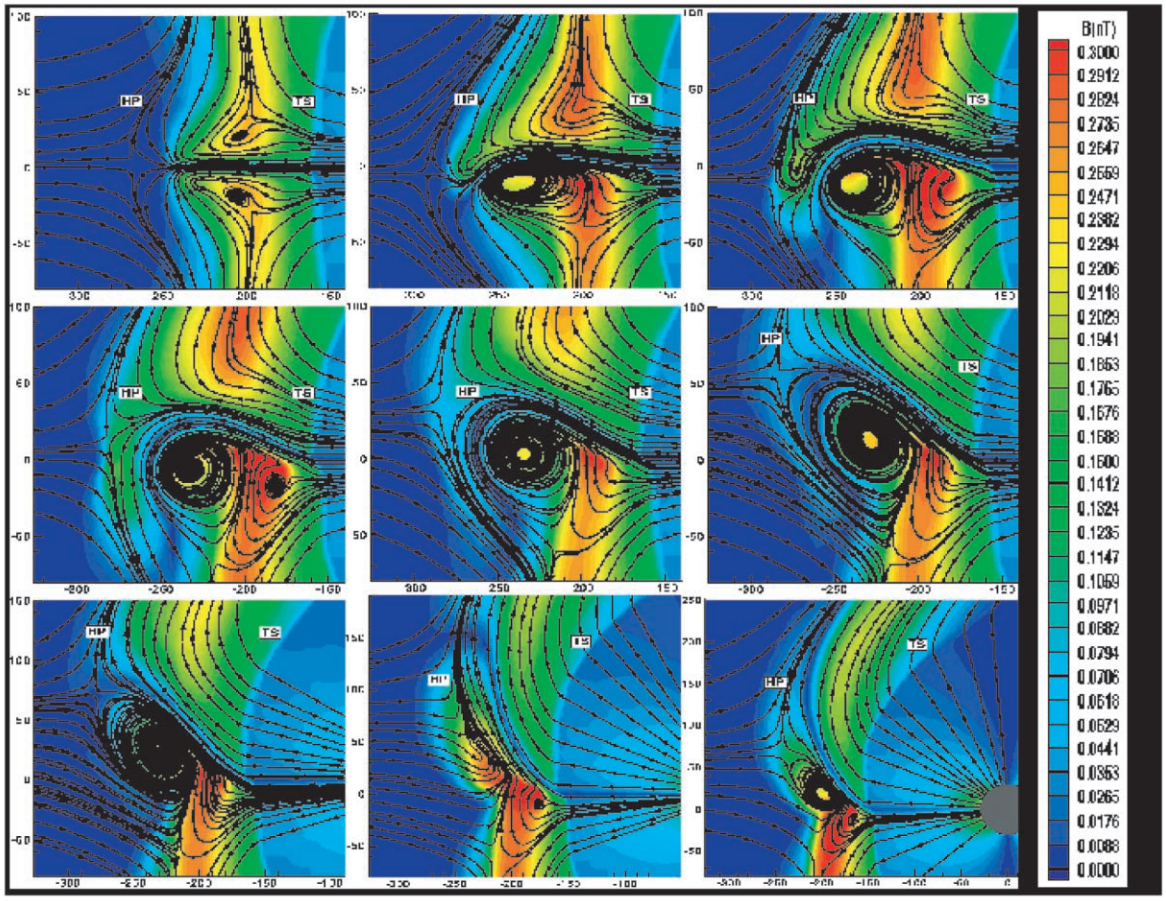

FIG. 3.—Time evolution of the current sheet instability; contours of the magnetic field between the TS and HP (scale ranging from 0 to 0.3 nT). The nine panels shown correspond to $t = 39.2$, 71.8, 89.8, 114.8, 200.0, 258.4, 278.5, 349.0, and 464.0 yr (*left to right, top to bottom*). The current sheet is bent to the south and subsequently to the north. [This figure is also available as an mpg animation in the electronic edition of the Journal.]

3. DISCUSSION

In the present study, we have neglected the effect of the tilt in the solar dipole (15° from the rotation axis), as in ud-Doula & Owocki (2002) and the previous heliospheric studies by Linde et al. (1998) and Washimi & Tanaka (1996). Time-dependent effects such as solar rotation (27 days) can affect our results. Because of the tilt between the magnetic and the solar rotation axis, the current sheet near the Sun takes the shape of a "ballerina skirt" and can change the region beyond the termination shock. We plan to investigate how this affects the instability. Past work has shown that the effect of the inclusion of the neutrals coupled to the plasma through charge exchange interactions has several effects, such as diminishing the distances to the TS, HP, and bow shock and affecting the heliospheric flow velocity. We intend to include self-consistently the neutrals to study their effect on the jet-sheet structure. The formation of an unstable jet-sheet at the edge of the solar system can potentially affect the entry of energetic particles and the intermixing of interstellar and stellar material.

The interaction between stellar winds and the interstellar medium produces several detectable astrophysical structures. Hydrogen walls have been observed in several nearby stars (Wood et al. 2001), including our own solar system (Linsky & Wood 1996). Stellar wind bow shocks have been observed on a wide variety of astrophysical scales and associated with pulsars (Cordes, Romani, & Lundgren 1993), OB-runaway stars (Van Buren & McCray 1988), and neutron stars (Chatterjee & Cordes 2002). We predict the formation of an unstable jet-sheet in other stellar systems as well. The necessary ingredient is a magnetized fast-rotating star possessing a supersonic wind that moves with respect to the interstellar medium. The probable candidates are rotating O stars with hot winds having high velocity with respect to the interstellar wind. The strength of the jet-sheet instability is proportional to the shear velocity between the flow at the current sheet and in the surrounding medium that is being slowed by the magnetic ridges. The intensity of the magnetic ridges depends on the magnetic field, the wind ram pressure, and the rotation rate of the star. Therefore, we predict that the instability will be enhanced for fast-rotating stars with strong magnetic fields. Because the compression of the stellar azimuthal field is also dependent on the interstellar pressure, the instability will be further enhanced for fast-moving stars relative to the interstellar medium.

We thank M. Velli for helpful discussions. Much of this work was performed at the Jet Propulsion Laboratory of the California Institute of Technology under a contract with NASA. The University of Michigan work was also supported by NASA. G. T. was partially supported by the Hungarian Science Foundation (OTKA; grant T037548).

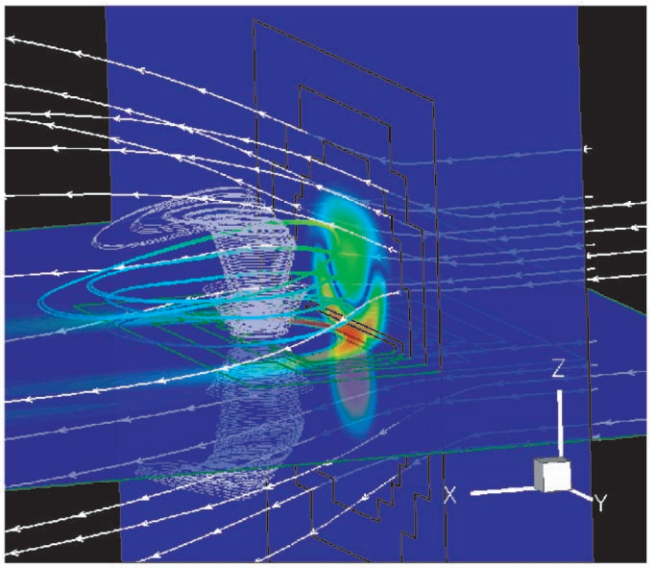

FIG. 4.—Three-dimensional image at $t = 346$ yr. The horizontal cut is the ecliptic plane ($z = 0$), and the vertical cut is at $x = -200$ AU. The purple lines show the Parker spiral bending backward toward the tail of the heliosphere. The green lines indicate the magnetic field lines being compressed by the termination shock. The contours of the magnetic field intensity are shown with the same scale as in Fig. 1. The blue region between the green zones denotes the current sheet as it seen from the nose of the heliosphere (a "smile shape"). Also shown in black (for the slice at $x = -200$ AU) and deep green (for $z = 0$) are the boundaries between regions of different refinement. The white streamlines are the flow streamlines.

REFERENCES

Baranov, V. B., & Malama, Y. G. 1993, J. Geophys. Res., 98, 15157
Chandrasekhar, S. 1961, Hydrodynamic and Hydromagnetic Stability (Oxford: Clarendon)
Chatterjee, S., & Cordes, J. M. 2002, ApJ, 575, 407
Cordes, J. M., Romani, R. W., & Lundgren, S. C. 1993, Nature, 362, 133
Frisch, P. C. 1996, Space Sci. Rev., 78, 213
Gombosi, T. I., Toth, G., DeZeeuw, D. L., Hansen, K. C., Kabin, K., & Powell, K. G. 2002, J. Comput. Phys., 177, 176
Izmodenov, V. V., Gruntman, M., & Malama, Y. G. 2001, J. Geophys. Res., 106, 10681
Landau, L. D., & Lifshitz, E. M. 1987, Fluid Mechanics (Oxford: Pergamon)
Liewer, P. C., Karmesin, S. R., & Brackbill, J. U. 1996, in AIP Conf. Proc. 382, Solar Wind Eight, ed. D. Winterhalter, J. T. Gosling, S. R. Habbal, W. S. Kurth, & M. Neugebauer (Woodbury: AIP), 613
Linde, T. J., Gombosi, T. I., Roe, P. L., Powell, K. G., & DeZeeuw, D. L. 1998, J. Geophys. Res., 103, 1889
Linsky, J. L., & Wood, B. E. 1996, ApJ, 463, 254
Müller, H.-R., Zank, G. P., & Lipatov, A. S. 2000, J. Geophys. Res., 105, 27419
Nerney, S., Suess, S. T., & Schmahl, E. J. 1991, A&A, 250, 556
———. 1993, J. Geophys. Res., 98, 15169
Parker, E. N. 1958, ApJ, 128, 664
Pauls, H. L., & Zank, G. P. 1996, J. Geophys. Res., 101, 17081
Pauls, H. L., Zank, G. P., & Williams, L. L. 1995, J. Geophys. Res., 100, 21595
Pogorelov, N. V., & Matsuda, T. 2000, A&A, 354, 697
Powell, K. G., Roe, P. L., Linde, T. J., & Gombosi, T. I. 1999, J. Comput. Phys., 154, 284
Stone, E. C., Cummings, A. C., & Webber, W. R. 1996, J. Geophys. Res., 101, 11017
Suess, S. T. 1990, Rev. Geophys., 28, 97
ud-Doula, A., & Owocki, S. P. 2002, ApJ, 576, 413
Van Buren, D., & McCray, R. 1988, ApJ, 329, L93
Washimi, H., & Tanaka, T. 1996, Space Sci. Rev., 78, 85
———. 2001, Adv. Space Res., 27, 509
Wood, B. E., Linsky, J. L., Müller, H.-R., & Zank, G. P. 2001, ApJ, 547, L49
Zank, G. P., Pauls, H. L., Williams, L. L., & Hall, D. T. 1996, J. Geophys. Res., 101, 21639